Environmental and Climate Technologies
2026, vol. 30, no. 1, pp. 232–250
https://doi.org/10.2478/rtuect-2026-0016
https://content.sciendo.com

RIGA TECHNICAL UNIVERSITY

Empirical Model for Predicting the Combustion Performance of Low-Quality Biomass Pellets Based on Experimental Data

Oskars SVEDOVS[1*], Haralds SIKTARS[2], Jana CERNEJA[3], Kristaps KASS[4], Taras MIKA[5], Vivita PRIEDNIECE[6], Edgars VIGANTS[7], Vladimirs KIRSANOVS[8]

[1–8]*Institute of Energy Systems and Environment, Riga Technical University, Azenes iela 12/1, Riga, LV-1048, Latvia*

Received 02.12.2025; accepted 18.03.2026

***Abstract* – Low-quality biomass (LQB) is an abundant feedstock for small-scale heat generation, but its variable composition often leads to unstable combustion and elevated emissions in domestic boilers. This study assesses the combustion behaviour of 18 pelletized LQB feedstocks using a 25-kW boiler operated under controlled conditions. The fuels exhibited wide performance differences, reflected in broad emission ranges and noticeable variation in thermal efficiency. To support predictive evaluation, statistical models were established that link key fuel characteristics with CO, NO_x, PM and efficiency, enabling quantitative estimation of combustion performance across heterogeneous feedstocks. To clarify ash-related effects, ten representative ashes were characterized using ICP-OES and XRD. Their chemical and phase compositions were assigned to the main Vassilev classes, which corresponded to distinct ash-forming mineral groups. Ca-rich ashes were dominated by carbonate and phosphate phases suitable for neutralization or construction applications. K-rich ashes contained soluble sulphate and chloride species relevant for nutrient-recovery routes, while Si-rich ashes consisted mainly of quartz or amorphous matrices with low reactivity. The combined combustion and ash elemental and phase analysis results demonstrate clear links between LQB composition, emission behaviour and ash transformation mechanisms, providing a practical basis for evaluating the suitability of alternative biomass pellets for small-scale heat production.**

***Keywords* – Alternative biomass; alternative pellets; biomass; combustion; domestic boiler; empirical model; low-quality biomass; pellets; prediction.**

* Corresponding author.
E-mail address: oskars.svedovs@rtu.lv

Oskars SVEDOVS https://orcid.org/0009-0006-1086-1076
Haralds SIKTARS https://orcid.org/0009-0007-3017-0464
Jana CERNEJA https://orcid.org/0009-0001-9260-4578
Kristaps KASS https://orcid.org/0009-0007-5165-2948
Taras MIKA https://orcid.org/0009-0000-2865-782X
Vivita PRIEDNIECE https://orcid.org/0000-0002-6894-4265
Edgars VIGANTS https://orcid.org/0000-0003-3408-5711
Vladimirs KIRSANOVS https://orcid.org/0000-0003-2501-5471

1. INTRODUCTION

Given that the basic principles of the bioeconomy (particularly the rational allocation and utilization of resources) have been successfully integrated into most forestry, agricultural and manufacturing subsectors, the demand for effective disposal and valorization technologies for low-quality biomass (LQB) has increased. These subsectors generate a broad range of LQB types, from pine needles and tree leaves to brewer's spent grains and sewage sludge [1]. In general, three technological pathways exist for LQB utilization: pre-treatment, conversion (particularly – direct combustion), and the application of intermediate biomass products [2].

Direct combustion essentially involves using LQB as fuel in an incineration plant for direct heat generation to increase the temperature of the circulating heat carrier. However, inappropriate quality indicators (e.g., increased moisture content [3]) can significantly impair combustion behaviour. Industry practice therefore commonly treats pelletization and torrefaction as quality improvement measures [4]. Additional thermochemical and biochemical conversion routes are available (gasification for syngas production [5] and anaerobic fermentation for biogas generation [6]) yet the capital intensity of such installations may jeopardize economic feasibility despite the low cost and wide availability of LQB feedstocks [7].

Although pellet production technologies have advanced considerably, the environmental performance of alternative (non-wood) biomass pellets remains insufficiently clarified [8]. In the residential heating sector, combustion takes place directly inside household stoves or boilers that often lack dedicated emission-reduction components [9]. Suboptimal operating conditions can further elevate pollutant formation, especially particulate matter (PM) [10]. PM emissions from domestic boilers are a documented and persistent problem in numerous countries [11]. Solving the problem commonly includes improving the fuel properties or construction of the boiler. Improving the boiler design involves integrating gas treatment technologies (e.g., a wet scrubber with a sustainable water treatment function [12]) into the standard system [13]. On the other hand, the pelletization mentioned above leads to an increase in the quality of the LQB and, respectively, a reduction in the concentration of PM and other emissions in the flue gas [14]–[16].

To enhance pellet combustion even further, boiler operators should adjust operating parameters to ensure more favourable in-furnace conditions. Such adjustments require experimental data that show how fuel properties influence combustion. In this study, the authors pelletized and analysed several LQB types and assessed their combustion performance. Previous studies performed by different authors have usually examined separate parts of this process (see Table 1). Some studies examine only fuel-related properties; Sommersacher *et al*. [17] link ash composition with slagging and corrosion behaviour by using several ash-based indicators such as the Slagging Index (SI). However, these studies do not include pellet mechanical quality or any aspects related to LQB preparation and logistics. Other research focuses on fuel-quality classification systems, such as the Biomass Quality Index (BQI) or Fuel Quality Index / Fuel Quality Label (FQI/FQL), but these approaches remain separate from actual combustion performance. Similar ranking approaches based on SI can be found as well. Studies that concentrate on the combustion stage normally analyse only the combustion process itself. Indicators such as Modified Combustion Efficiency (MCE) or the CO/CO_2 ratio are used to characterize combustion behaviour and emissions, yet these works do not include detailed fuel characterization or pellet properties. On a broader level, diagnostic emission ratios (CO/NO_x, SO_2/NO_x, NO/NO_2) are applied in atmospheric studies to interpret emission origin, but they are not directly linked to specific pellet types, combustion regime or fuel quality.

TABLE 1. EXISTING STUDIES ON THE INTRODUCTION AND VALIDATION OF BIOMASS QUALITY AND ITS COMBUSTION INDICATORS

Type of research	**Indicator**	**Purpose**	**Source**
Raw material analysis/ Combustion analysis	SI	Slagging/ corrosion prediction	Sommersacher *et al*., 2011 [17]
Raw material analysis	BQI	Ranking	Rocha *et al*., 2019 [18]
Raw material analysis	FQI/FQL	Classification	Vasileiadou *et al*., 2021 [19]
Raw material analysis	SI	Ranking	Nik Norizam *et al*., 2023 [20]
Combustion analysis	MCE	Efficiency	Tian *et al*., 2015 [21]
Combustion analysis	CO/CO_2	Efficiency, emissions	Narnaware & Pareek, 2015 [22]
Combustion analysis	CO/CO_2	Regime analysis	Anca-Couce *et al*., 2017 [23]
Combustion analysis	CO/CO_2	Efficiency, emissions	Osei *et al*., 2020 [24]
Air quality analysis (direct biomass combustion impact)	CO/NO_x, SO_2/NO_x, NO/NO_2	Emission source identification	Abdul Halim *et al*., 2018 [25]
Air quality analysis (direct biomass combustion impact)	CO/NO_x, SO_2/NO_x	Emission source identification	Al-Dabbous, 2025 [26]
Air quality analysis (indirect biomass combustion impact)	SO_2/NO_x	Emission source identification	Nirel & Dayan, 2001 [27]

There is a clear methodological gap: a lack of integrated studies that follow the full sequence from LQB feedstock properties, pellet quality, combustion performance and emission profiles. These elements directly influence each other in low-capacity boilers, especially when using heterogeneous and ash-rich biomass. A unified experimental dataset combining all stages would allow a more complete understanding of how LQB properties affect combustion and emissions.

The present article addresses this gap by analysing the full chain using experimental data and empirical modelling approaches within the framework of the Bioenergy Observatory project. This integrated approach allows linking fuel properties with combustion results and provides a practical basis for predicting combustion behaviour from measurable fuel parameters.

2. METHODOLOGY

The study is an experiment that tests full spectrum of 18 biomass pellets samples. The basic experiment structure is shown in Fig. 1. The biomass preparation consists mainly of three grinding stages (depending on the initial biomass fraction) and sieving. The authors pelletized biomass samples in different proportions combining with wood sawdust (see Subsection 2.2), subjected samples of raw biomass and pellets to fuel testing with specialized equipment (see Subsection 2.1) and stored the pellets in the laboratory under controlled indoor environmental conditions. The authors conducted combustion tests on the samples using specialized equipment (see Subsection 2.3). Additionally, the authors performed statistical post-processing (see Subsection 2.4), where regression analysis was used to link fuel properties, pellet characteristics and combustion-stage indicators. For ash characterization, chemical and phase analyses were conducted for 10 out of the 18 pellet samples, each treated individually

to preserve sample specificity (see Subsection 2.5). Collected ash from these 10 tests was analysed by Inductively Coupled Plasma-Optical Emission Spectroscopy (ICP-OES) and powder X-ray diffraction (XRD) to integrate bulk chemistry with crystalline phase information and to evaluate potential utilization pathways (e.g., as a cement additive, fertilizer, or for neutralization).

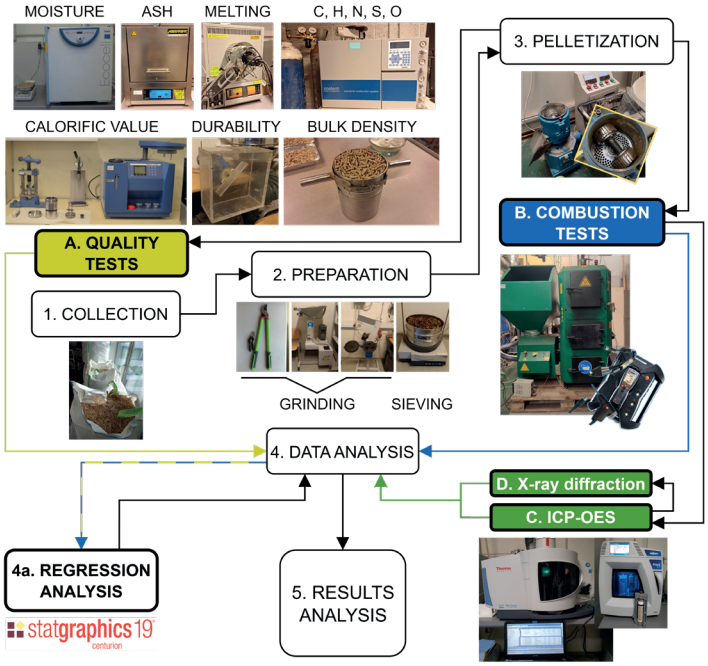

Fig. 1. Principial scheme of research framework.

2.1. Biomass Preparation and Testing of Fuel Properties

The authors performed biomass preparation at the Riga Technical University (RTU) Institute of Energy Systems and Environment (IESE), Environmental Monitoring Laboratory (EML), and identified the defining properties of all samples as summarized in Table 2. Main proximate analysis representative parameters – moisture content (MC) and ash content (AC) – were determined because both parameters fundamentally affect the subsequent processing of the raw biomass. For pellets, MC is a critical operational parameter: elevated MC increases the energy required for water evaporation and reduces combustion efficiency. Bulk density (BD) is relevant primarily from a logistical and economic perspective, as higher BD combined with higher net (NCV) or gross calorific value (GCV) results in greater energy density. Durability (DU) determines the mechanical stability of pellets during handling, transport and storage; pellets with insufficient DU tend to fragment, generating dust, increasing fire risk and compromising combustion stability. The ash melting point (AMP) indicates the tendency of ash to form slag, which may lead to fouling, deposits and structural damage within the boiler. These parameters are also used to categorize pellet quality in ISO 17225-6:2021 [28]. Ultimate analysis, which includes the determination of carbon (C), hydrogen (H), nitrogen (N), sulphur (S) and oxygen (O) content (CHNS-O), had also been conducted on selected samples with laboratory equipment – these data were used for the determination and verification of the NCV established by another method.

TABLE 2. BIOMASS QUALITY PARAMETERS MEASURED, METHODS AND EQUIPMENT USED

Parameter	Method used	Equipment used
MC, wt.%	LVS EN ISO 18134-2:2017	Ecocell 55; Ecocell 111
AC, wt.%	LVS EN ISO 18122: 2023	SNOL 7.2/1300; Nabertherm LT5/14; Nabertherm P320
DU, %	LVS EN ISO 17831-1:2016	Motovario HA 42
BD, kg/m^3	LV EN ISO 17828:2016	Metal measuring cup (5 L)
NCV, kJ/kg	LVS EN ISO 18125: 2017	IKA C2000 basic
GCV, kJ/kg	LVS EN ISO 18125: 2017	IKA C2000 basic
AMP, °C	EN ISO 21404:2020	Carbolite CAF DIGITAL
CHNS-O, %	LVS EN ISO 16948:2015	Costech ESC 4010

2.2. Production of Biomass Pellets

A D-type ZLSP200B pelletizer was used to produce biomass pellets for experimental purposes, with a productivity of 80–120 kg h^{-1}. The device consists of two parts: a mechanical part (rollers, die and knife) and an electrical part (motor, control console and circuit breaker). The console activates the motor, which rotates the die (a 6 mm die was used). Friction between the rotating die and the rollers increases the temperature of the mechanical assembly, with typical operating temperatures of approximately 90 °C. The knife cuts extruded pellets to the required length.

TABLE 3. BIOMASS PELLET SAMPLES CREATED AND TESTED

Wood:Biomass proportion in pellets			
100:0	**60:40**	**50:50**	**0:100**
P1: ENPlus A1 pellets*	P3: Cotton textile waste	P4: Buckwheat hulls	P15: Brewer's spent grain
P2: Wooden sawdust		P5: Coffee grounds	P16: Sunflower husk pellets*
		P6: Apple pomace	P17: Hay pellets*
		P7: Wheat straw	P18: Spruce needles
		P8: Hemp stalks	
		P9: Reed	
		P10: Grain residues	
		P11: Canada goldenrod	
		P12: Mixed tree leaves	
		P13: Mown grass	
		P14: Peat	

* Premade (purchased) pellets were tested

Pellet production was carried out in small laboratory batches to supply the pellet boiler for 3-hour tests (see Subsection 2.3). The boiler consumes approximately 5 kg h^{-1}, and an additional ~5 kg is required for the stabilization phase before measurements begin, resulting in a total of ~20 kg of pellets per test. A key factor in pelletization is lignin content, which

varies between biomass types. Therefore, an experimental pelletizing approach was applied to ensure that produced pellets were visually free of cracks and mechanically durable. Pellet cracking and overall quality are directly dependent on MC [29]. Additional variation in pellet properties may arise due to raw-material heterogeneity and biomass seasonality.

Before pellet production, crushed biomass (particle size < 1–5 mm) was mixed with wood sawdust, typically in a 50:50 mass ratio (see Table 3). Some samples consisted of non-wood pellets or mixtures with lower wood content. The biomass and sawdust mixture was homogenized and adjusted to a target MC of 14–20 wt.%. The pelletizer manufacturer recommends an MC range of 12–18 wt.%, although different biomass types may require different levels. In this study, the overall target MC for pelletizing was approximately 18 wt.%. Individual MC values for biomass and sawdust were measured beforehand and based on an initial MC of ~8 wt.%, approximately 1 kg of water was added per 10 kg of mixture to achieve workable pelletizing conditions.

2.3. Experimental Configuration and Data Collection

The authors carried out the biomass pellets combustion tests at the RTU IESE Combustion Research laboratory (CRL). Fig. 2 illustrates the design of the experimental setup. The base of the setup is a pellet boiler GRANDEG GD BIO 25 kW (G) in which the combustion process took place. Boiler is located on scales DINI ARGEO DFW06 (E) for weight monitoring. The boiler is in semi-automatic mode, requires manual ignition of the fuel in the burner (H) and can only then be switched to automatic control. An automation unit SKA1200025 with a power of 0.25 kW (D), is designed to maintain the speed and torque of smaller motors by varying motor speed based on preset system parameters. Successful demand requires a CT Comms cable USB – RS485 (C), which allows the automation unit to communicate with the converter on the PC for programming and monitoring. SyPTLite software was used for communication purposes. Looped ladder diagrams are required for a specific program. This feeder logic involves a time block. The timer is configured with the desired delay input in microseconds, and when conditions are met, the timer activates the output, which controls the motors. The ladder diagram consists of multiple sections of code.

Screw Feed input or auger feeder (B) is the primary control for mechanisms used to deliver test pellets to the heating boiler from the pellet bunker (A). Besides automatically controlling auger feeder with SyPTLite, also manual operation mode is possible, which is used for preparation or post-test cleaning. Input signals represent operation modes to ensure the auger feeder only operates under desired conditions; this section controls pulse width modulation (PWM) for regulating seed of duty cycle, input data is desired pellet feeding timer in microseconds (how long pallets are going to be fed in the system), our input is to after every 44 000 μs feed pallets for 4000 μs.

An air fan (F) ensures proper combustion conditions, this code section manages the operations of a fan for airflow conditions combined with a control signal to turn the fan on/off, in our case timer input is to after every 5000 μs turn on the fan and burst air flow into the burner. Besides air supply fan, also airduct draft removes flue gases from the burner, thus creating a better environment for combustion. Draft was manually regulated to be around –10 Pa using airduct valve (J). However, if air supply fails, it may cause safety hazards, similarly is with water pump (I), which provides cooling function of the boiler, thus preventing the overheating. Therefore, safety signals monitor critical system parameters like motor overload and pallet feed status. If input conditions are met, the system activates an alarm or stops operation completely.

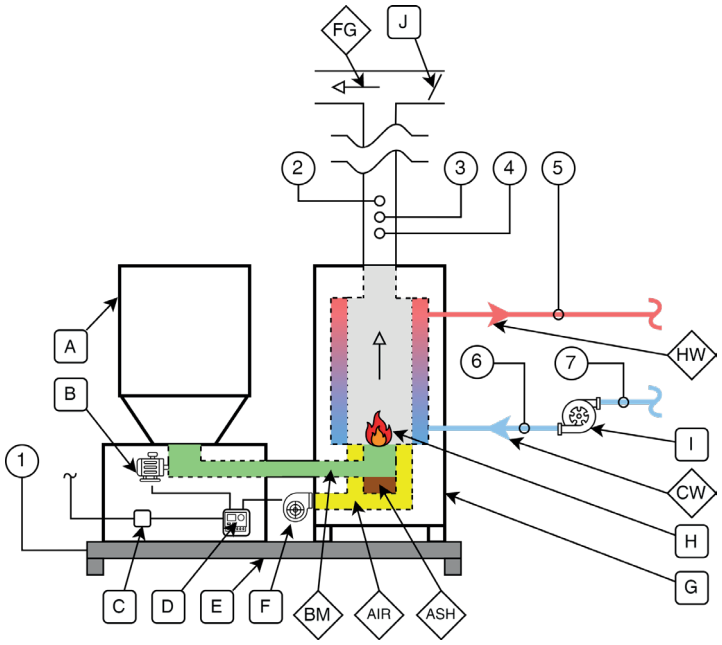

Fig. 2. Scheme of experimental setup. BM – Pellet supply; AIR – Air supply; ASH – Ash collecting chamber; CW – Cold water flow; HW – Hot water flow; FG – Flue gas flow.

Combustion and boiler parameters were measured and collected using invasive and non-invasive methods, with probe locations numbered from 1 to 7. For details on the measurement devices, see Table 4.

TABLE 4. BIOMASS COMBUSTION PARAMETERS MEASURED, METHODS AND EQUIPMENT USED

Sign	Parameter	Method used	Equipment used
4	Flue-gas temperature, °C	EN 14789:2017	Testo 350 (TC Type K)
4	O_2 content in flue-gas (O_2), %		Testo 350
4	CO content in flue-gas (CO), ppm	EN 15058:2017	
4	NO_x content in flue-gas (NO_x), ppm	ISO 10849:2022	
3	PM content in flue-gas (PM), mg/m^3	VDI 4206-2	Testo 380
1	Pellet consumption, kg	EN 45501-8.3	DINI ARGEO DFW06
2	Pressure gauge, Pa	EN 303-5+A1:2023	DPT FLOW 2000
6	Inlet water temperature, °C		Campbell Scientific TC 108
5	Outlet water temperature, °C		
7	Water volumetric flow, l h^{-1}		Kamstrup MULTICAL 602
–	Input power, kW		–
–	Output power, kW		–
–	Boiler efficiency (ζ), %		–

Data collection and logging was organized with Campbell Scientific measurement and control data logger CR1000, which had additional extension of AM16/32B Channel Relay Multiplexer and corresponding software – LoggerNet 4.4.2. Logged data was analysed in Microsoft Office Excel. Flue gas composition data was logged by Testo EasyEmision software and PM with Testo EasyHeat software. Water volumetric flow was read manually from Kamstrup MULTICAL 602 every hour, similarly, pellet consumption was read from scales DINI ARGEO DFW06. Also, ambient conditions (relative humidity (RH), ambient temperature (AT) and atmospheric pressure (AP)) were monitored hourly using Testo 622. Combustion tests were conducted on similar conditions for every sample, since ambient parameters were not drastically changed throughout the tests, therefore changes in ambient conditions are considered insignificant in this experiment. The beginning point of the test was the moment when the boiler works steadily and the inlet and outlet water temperatures have stabilized, as well as changes in flue-gas composition, flue-gas temperature and output power are stable or have low fluctuations.

2.4. Regression Analysis

The data obtained from the experimental study were analysed using regression analysis. Regression analysis provides a universal framework for identifying quantitative relationships among variables and for constructing predictive models with improved reliability. Regression outputs are frequently used as the basis for empirical models, for example, for predicting pellet durability [30] and boiler efficiency [31]. The analytical workflow included comprehensive data pre-processing, involving data cleaning, handling missing observations, detection of anomalous values, and data normalization to ensure the integrity of the input dataset. Subsequent exploratory data analysis was performed to characterize variable distributions, reveal underlying trends, and evaluate multicollinearity using correlation matrices and variance inflation factors. All statistical computations within this study were conducted in STATGRAPHICS Centurion 19.

2.5. ICP-OES and XRD Analysis

An ICP-OES was used for quantitative multi-element characterization of biomass ash because of its advantages like simultaneous detection of large variety of elements , a broad linear dynamic range Quantification followed LVS EN ISO 16967:2015 [32] for major elements and LVS EN ISO 16968:2015 [33] for minor/trace elements to ensure traceability and inter-laboratory comparability.

Analyses were performed on a Thermo Scientific iCAP 7400 ICP-OES. The sample introduction comprised a PTFE cyclonic spray chamber and a Burgener Mira Mist nebulizer (gas flow rate 0.65 L min^{-1}). Peristaltic pump operated at 50 rpm for stable uptake and rinsing (sample: TFS white/white; drain: TFS yellow/blue). Dual-view acquisition was used with representative integration times of 15 s in the ultraviolet and 10 s in the visible spectral range both operated at 1150 W radio-frequency power. Ashes were mineralized in sealed PTFE vessels (MARS 6 with EasyPrep) using nitric acid (HNO_3) and hydrofluoric acid (HF) with hydrogen peroxide (H_2O_2) as oxidant at elevated temperatures accordingly to the standard procedures. After digestion, boric acid (H_3BO_3) was added to complex residual fluorides to avoid damage of quartz compartment during ICP-OES measurements (a 2 mm ceramic nozzle was used). High-purity acids and ultrapure water (Barnstead MicroPure) were used to minimize contamination and ensure reproducible dilutions. External calibration was based on Multielement Standard Solutions V (p/n 54704) and VI (p/n 43834) to span the expected analyte ranges; cysteic acid monohydrate was used as the sulphur standard.

Powder XRD was performed on a Bruker D8 Advance diffractometer in Bragg-Brentano geometry (Cu anode with Ni filter; scintillation detector). XRD patterns were collected in 2θ range from 10° to 80° at a continuous scan speed of 0.01 ° s^{-1}. Crystallography Open Database (COD) [34], [35] was used for phase identification and semi-quantitative phase analysis was done by Rietveld refinement using BGMN via Profex v5.5.2 [36].

ICP-OES results of elemental composition were expressed as oxides. They were normalized to 100 % and assigned to classes on a rule-based ternary diagram developed by Vassilev [37]–[39]. The class inferred from ICP-OES provided prior expectations for candidate phase fields and approximate glass fraction, which informed the XRD phase list and interpretation. The observed XRD assemblage then tested and refined those expectations. Together, the ternary placement and the XRD results supported material-routing decisions, for example distinguishing salt-rich ashes with potential for nutrient recovery from Ca-/Si-dominated ashes suitable for neutralization or supplementary cementitious applications.

3. RESULTS

Applying the methodology described yielded results on the quality of the samples and the combustion process. Several combustion tests were repeated for certain samples, as the initial ones revealed an inadequate operating regime. This occurred because the boiler used in the experiments is not equipped with a lambda probe, making automatic adjustment of the regime impossible. The validated and reliable data are summarized below, and these data were used for the regression analysis.

3.1. Quality Tests Results

Pellet quality indicators demonstrate substantial heterogeneity across the samples analysed as seen in Table 5. MC ranges from 3.69 wt.% (P3) to 13.30 wt.% (P14), reflecting differences in biomass structure and drying behaviour, although most samples fall near the expected air-dry level of ~9–10 wt.%. AC exhibits the widest variability – from 0.37 wt.% (P1) to 7.37 wt.% (P17). Based solely on AC thresholds defined in ISO 17225-6:2021 (Class A: < 3 wt.%; Class B: 3–6 wt.%; Class C: 6–10 wt.%), the pellets can be grouped into: Class A (P1, P2, P3, P4, P6, P10, P14), Class B (P5, P7, P9, P11, P15, P16, P18), Class C (P8, P12, P13, P17). DU varies from 91.7 % to 98.8 %, with ISO Class A requiring DU ≥ 96 %; several samples fall below this threshold, indicating weaker mechanical stability (P6, P7, P8, P11, P12, P15, P17, P18). BD varies 390–740 kg m^{-3}; only P1, P2, P3 and P18 of the samples meet the ISO Class A/B range of 600–750 kg m^{-3}, with lower-density pellets being characteristic of non-woody biomass. NCV lies between 16.08–19.04 MJ kg^{-1}, with only pellets above 16.5 MJ kg^{-1} (P1, P2, P3, P4, P5, P9, P12, P14, P15, P16, P18) meeting the minimum requirement for Class A fuels.

TABLE 5. RESULTS OF PELLETS QUALITY TESTS

Pellet type	MC, wt.%	AC, wt.%	DU, %	BD, kg m^{-3}	NCV, MJ kg^{-1}	GCV, MJ kg^{-1}	AMP, °C
P1	9.80	0.37	98.4	700	18.13	20.91	1412
P2	5.10	0.72	96.9	640	18.72	21.21	1295
P3	3.69	1.56	98.8	740	17.70	19.84	1200
P4	11.52	1.39	97.3	540	16.76	20.51	1079
P5	8.60	4.25	97.7	554	19.04	20.53	1320
P6	10.00	1.17	95.4	526	16.36	19.79	1070

P7	9.39	4.22	92.9	520	16.35	19.65	1020
P8	10.55	6.00	92.4	453	16.42	19.88	1422
P9	7.05	3.73	94.9	580	17.33	20.40	1096
P10	9.72	1.52	97.6	525	16.40	19.86	1041
P11	12.88	3.76	91.7	390	16.39	20.56	1102
P12	9.20	6.51	95.8	500	16.97	20.24	1208
P13	12.02	6.32	96.0	520	16.34	20.27	1128
P14	13.30	1.28	97.1	518	16.73	21.04	1156
P15	9.70	3.96	92.1	570	17.65	21.29	1480
P16	9.10	3.40	97.8	498	17.00	20.30	1125
P17	4.24	7.37	92.8	570	16.08	18.21	1020
P18	4.26	5.50	92.9	611	17.87	20.12	1162

3.2. Combustion Tests Results

AT were ranged from 21.9 °C to 25.1 °C, RH were ranged 23.7–48.0 %, AP were ranged from 1000.5 hPa to 1044.0 hPa. Combustion tests results are shown in Table 6. For each test the expected O_2 was 10 %, however, fluctuations were observed – the highest amount of O_2 was for P11 (11.2 %) and the lowest amount of O_2 was for P15 (8.2 %). By CO pellets can be divided into three categories: (1) up to 1000 mg Nm^{-3} (P1, P2, P8, P10, P14), (2) from 1000 to 10 000 mg Nm^{-3} (P3, P5, P6, P9, P11, P12, P15) and (3) above 10 000 mg Nm^{-3} (P4, P7, P13, P16, P17, P18).

TABLE 6. RESULTS OF PELLETS COMBUSTION TESTS

Pellet type	**O_2, %**	**CO, mg Nm^{-3}**	**NOx, mg Nm^{-3}**	**PM, mg Nm^{-3}**	**ζ, %**
P1	9.1	244	337	22	83.0
P2	10.4	52	140	21	80.4
P3	8.6	5416	343	68	79.6
P4	10.6	14 750	780	211	72.4
P5	11.0	7425	429	87	69.4
P6	9.2	2796	349	66	78.4
P7	10.8	20 416	192	176	68.0
P8	11.0	646	189	161	77.3
P9	9.0	3421	677	143	72.7
P10	8.7	800	600	37	78.5
P11	11.2	7648	525	139	74.1
P12	10.5	9827	369	139	70.5
P13	10.6	14 750	780	211	72.4
P14	10.8	664	517	54	79.7
P15	8.2	7288	948	177	80.4
P16	9.7	29 237	353	104	66.3
P17	10.7	48 238	786	218	68.0
P18	10.5	23 261	718	122	70.5

(1) category had sufficient combustion and proper mixture ratio between fuel and air. Indications of incomplete combustion can be observed in (2) category, which happen due to insufficient mixing of fuel and air and insufficient O_2 supply. (3) category requires different designs of boiler (e.g., with secondary air modification [40]) or other conversion technology. Both purchased (P1) and made (P2) wood pellets showed practically the same average values for PM 22 mg Nm^{-3} and 21 mg Nm^{-3}, respectively. The average PM concentration of other fuels in flue gases is up to 218 mg Nm^{-3}. ζ varies between 66.3 % and 83.0 %, lowest values observed for (3) category. Overall, besides wood pellets, samples P10 and P14 are promising in terms of direct combustion and the resulting emissions.

The combustion test results of the pellets were compared with the requirements of Commission Regulation (EU) 2015/1189, which specify $\zeta \geq 77$ %, PM ≤ 40 mg Nm^{-3}, $NO_x \leq$ 200 mg Nm^{-3} and CO ≤ 500 mg Nm^{-3}. These regulatory requirements apply to boiler operation when the manufacturer specifies the use of LQB pellets in the boiler. According to the results, only P2 fully complies with all the criteria for use in the tested boiler. P1, P2, P3, P6, P8, P10, P14 and P15 meet minimal requirements for ζ. P1, P2 and P10 meet minimal requirements for PM. P2, P7 and P8 meet minimal requirements for NO_x. P1 and P2 meet minimal requirements for CO.

3.3. Slag Formation

After the combustion tests were concluded, pellet boiler was cleaned from ash and slag, which later was visually analysed (see Fig. 3).

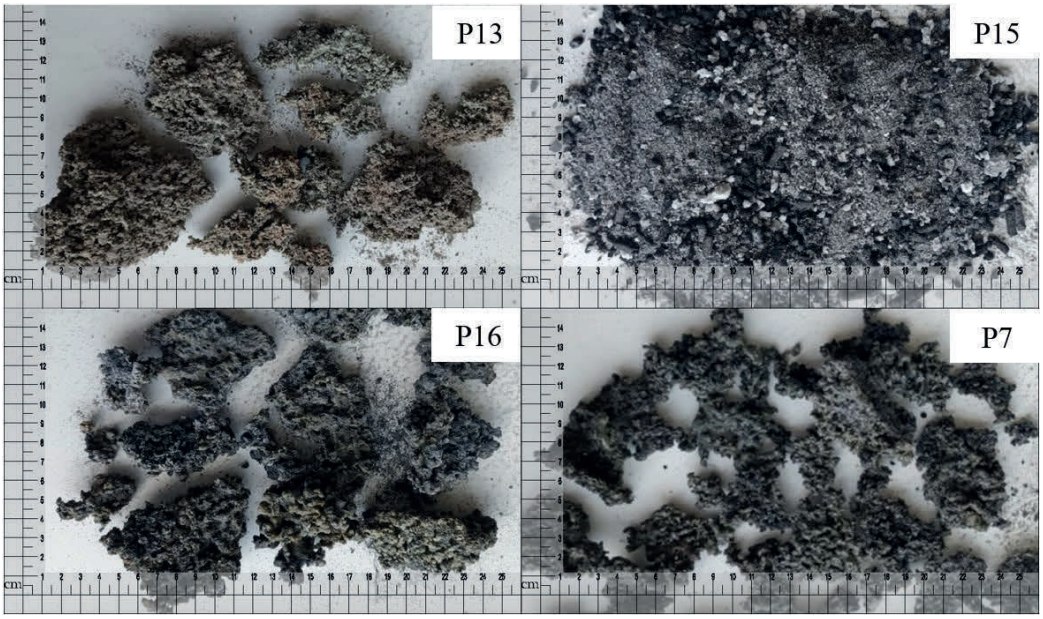

Fig. 3. Visual comparison of slag formation during LQB pellet combustion.

Samples shown (P7, P13, P15, P16) had the most problematic combustion process due to slag formation or ash amount. Physical properties, such as size, fragility, colour, weight, of slag differs, however slag formation amount is complicated to representatively indicate, but it is worth mentioning that P6 sample had significantly more slag formations, than other samples, whilst other samples had no considerable problems on combustion due to airway

clogging or ash melting. P13 did not form the slag, however, it showed large amounts of white impurities in the ashes and a part of the unburnt fraction remained after the combustion process. Colour differences indicates that chemical composition is different, whilst fragility of the slag formation was different between the samples, which also indicates different chemical composition, therefore different AMP.

3.4. Empirical Models

Four empirical models were elaborated using STATGRAPHICS Centurion 19: the independent and dependent variables selected for all models are given in Table 7. The dependent variables are the parameters characterizing the combustion process, while the independent variables are the fuel parameters. The empirical models partly include parameters shown in Table 1 because their impact on dependent variables is negligible. Empirical models for other dependent variables showed a low correlation between measured and predicted variables; therefore, only those with a determination coefficient (R^2) of ≥ 0.5 were selected by the authors.

TABLE 7. EMPIRICAL EQUATIONS DERIVED FROM REGRESSION ANALYSIS OF COMBUSTION PROCESS PARAMETERS

Parameter	Empirical model	R^2
CO	–118519 – 43.30 · AMP + 3994.56 · AC – 3445.35 · C	0.70
NO_x	228.79 + 158.85 · N + 2.66443 · AC	0.53
PM	23.24 + 25.14 · AC	0.52
ζ	97.55 – 1.88 · AC – 2.63 · NCV + 0.02 · AMP	0.74

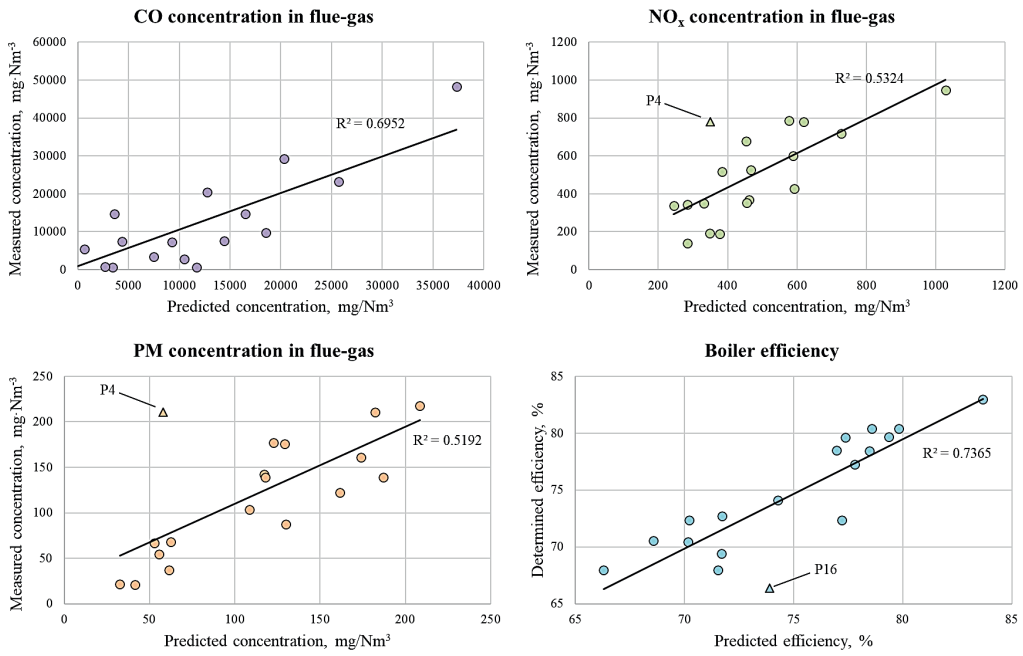

Fig. 4. Trend charts for measured and predicted values of dependent variables.

Fig. 4 presents the dependency diagrams between the measured CO, NO_x, PM and ζ values listed in Table 6 and the predicted values calculated using the equations shown in Table 7. All data points were included by the authors; however, sample P4 is clearly an outlier in the NO_x and PM cases, and sample P16 deviates in the case of ζ. According to regression theory, individual points may be omitted when they fall outside the expected trend. Therefore, these samples could be considered for exclusion, which might increase the R^2 values.

3.5. ICP-OES and XRD Results

ICP-OES and XRD analyses were performed for samples P2, P4, P7, P8, P9, P11, P12, P13, P15, and P16, as these represent four biomass groups distinguished by sector or origin: forestry (P2), agriculture (P7, P8, P9), food-processing residues (P4, P15, P16), and invasive or low-grade biomass (P11, P12, P13). Fig. 5 presents the rule-based ternary Vassilev diagram, which assigns each sample to a compositional class based on the relative proportions of major oxide groups.

The classes are defined by proximity to the diagram apices and boundaries. The C-class corresponds to calcareous ashes dominated by Ca-group oxides. The K-class identifies potassic or salt-rich ashes where K-bearing oxides and acid-soluble components prevail. The S-class denotes silica-dominated ashes with a strong framework-forming oxide fraction. The CK-class describes mixed calcareous-potassic compositions, typically characterized by high soluble K content and the presence of K-Ca double carbonates. The "-MA" subclasses (C-MA, K-MA, S-MA) indicate positions shifted toward the aluminosilicate apex, reflecting partial modification by mineral additives or naturally higher levels of Si-, Al-, or Fe-oxides, which increases ash refractoriness and suppresses low-melting behaviour.

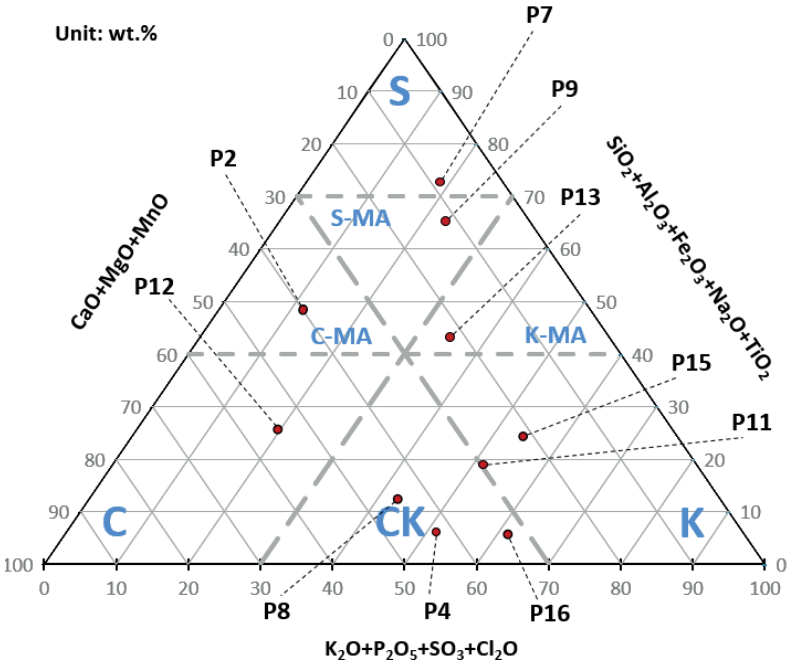

Fig. 5. Classification of biomass ashes in the Vassilev ternary diagram based on major oxide groups.

Table 8 summarizes the oxide composition of all analysed ash samples, presented without normalization to 100 % to allow direct comparison with the XRD-derived phase composition. The symbol "–" denotes minor oxides detected only at trace levels, which were excluded from comparison because they do not influence the classification of ashes. The data confirms clear differences among the compositional classes indicated in the Vassilev diagram. Samples assigned to the C and C-MA classes exhibit the highest CaO contents together with moderate MgO and relatively low alkali levels, consistent with a predominantly calcareous ash chemistry. CK-class samples contain markedly elevated K_2O combined with CaO and MgO, reflecting the presence of double K-Ca carbonate and sulphate phases. K-class samples show the greatest alkali and P_2O_5 enrichment, indicating strong phosphate accumulation in food-processing residues. In contrast, S and S-MA samples display the highest SiO_2 fractions and only minor CaO, reflecting a silica-dominated matrix with limited alkalinity.

TABLE 8. ELEMENTAL OXIDE COMPOSITION OF BIOMASS ASH SAMPLES

Sample	**P12**	**P2**	**P4**	**P16**	**P8**	**P11**	**P15**	**P13**	**P7**	**P9**
Class	**C**	**C-MA**	**CK**	**CK**	**CK**	**K**	**K**	**K-MA**	**S**	**S-MA**
Chemical element oxides, wt.%										
Al_2O_3	0.6	1.7	0.6	0.4	0.3	0.6	0.1	1.4	3.6	0.2
CaO	34.6	21.2	14.3	12.8	28.0	19.2	7.7	12.8	5.1	6.3
Fe_2O_3	0.3	3.7	–	–	–	0.5	1.7	0.9	1.5	0.4
K_2O	6.4	4.6	22.4	28.4	14.2	26.1	3.7	14.1	10.7	8.9
MgO	4.5	5.9	13.9	7.3	6.6	5.0	9.3	5.4	2.1	2.5
MnO	0.1	1.6	–	–	–	–	–	–	0.4	2.6
P_2O_5	5.2	2.5	9.4	3.9	16.5	11.1	40.2	11.5	2.3	5.3
SO_3	2.8	1.3	3.1	6.1	3.0	2.7	0.5	3.2	2.3	5.4
SiO_2	17.2	29.2	1.7	2.4	9.4	17.1	17.2	32.8	53.7	52.4
Na_2O	–	–	–	–	–	–	–	–	0.4	2.6
Total	72.4	72.7	67.7	62.7	78.6	83.1	82.1	83.0	82.0	84.6

Fig. 6 presents the XRD patterns of the investigated biomass ashes, illustrating formation of crystalline and amorphous phases after combustion. The diffractograms provide qualitative identification of major and minor mineral components, allowing differentiation between carbonate-, silicate-, phosphate-, and chloride- or sulphate-bearing phases. Reflections from each individual phase are marked with corresponding symbols to facilitate comparison of features across feedstocks for each ash type. The XRD patterns also reveal differences in crystallinity and the presence of amorphous phase, which are important for assessing ash transformation behaviour, melting tendencies, and potential utilization routes.

Table 9 presents the phase composition of the analysed ashes. The order of discussion below follows the column order of Table 8 to ensure full consistency. The symbol "-" denotes that the corresponding phase was either not detected or does not apply to the specific sample.

P12 and P2 contain $CaCO_3$ as the dominant phase, together with small amounts of SiO_2, K_2SO_4 and $Ca_5(PO_4)_3OH$. These phases correspond to the Ca-rich composition typical for C and C-MA classes, where $CaCO_3$ predominates and Si occurs mainly as quartz.

P4 contains K_2SO_4, $K_2Ca(CO_3)_2$ and $Ca_5(PO_4)_3OH$, reflecting its elevated K, Ca and P content. P16 shows a similar CK-type assemblage dominated by K_2SO_4 and $K_2Ca(CO_3)_2$ with a smaller amount of $Ca_5(PO_4)_3OH$. These samples represent typical CK chemistry, in which

potassium promotes the formation of double K-Ca carbonate phases. P8 contains higher amounts of $CaCO_3$ and $Ca_5(PO_4)_3OH$ than P4 and P16 and includes SiO_2. This agrees with its higher Ca, P and Si contents in comparison to the other CK samples.

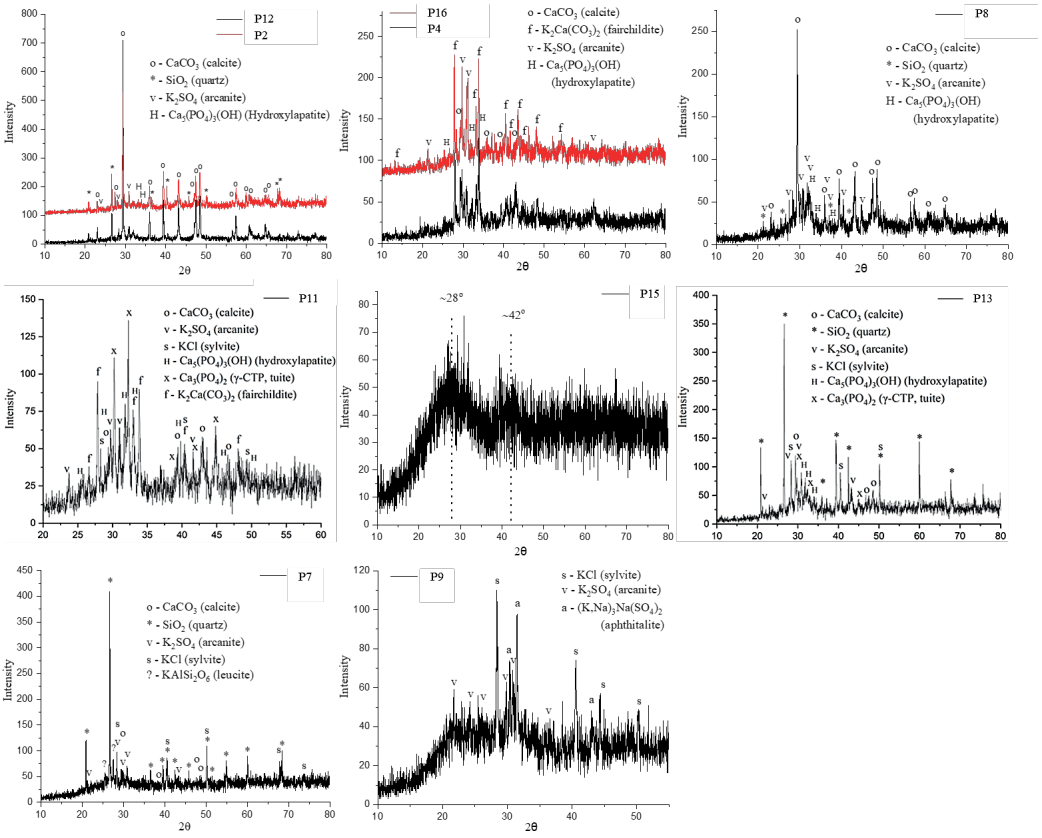

Fig. 6. XRD patterns for samples included in elementary analysis.

P11 contains $K_2Ca(CO_3)_2$, K_2SO_4, $Ca_5(PO_4)_3OH$, γ-$Ca_3(PO_4)_2$ and a small amount of KCl. Table 9 also shows a high amount of amorphous phase (marked "+"). This combination of mixed carbonates, sulphates, phosphates and a glassy component reflect its transitional position between CK and K classes. P15 shows no crystalline phases, and Table 9 indicates only an amorphous phase. The first amorphous halo appears at ~28°, the second one at ~42°. Elemental analysis shows that main component of ash is phosphorus and silica oxides. Using Braggs' formula [41] this gives dominant distances ~3.18 Å (main halo) and ~2.15 Å (secondary halo). The first, dominate distance, most probably is related to P-P bonds. Typically, this distance is 2.95–3.08 Å in an oxygen-bridged tetrahedra (P-O-P) in a phosphate glass [42]. Si-Si distance (~3.1 Å) fits well this medium-range order (Si-O-Si). The second distance (reflects short-range ordering) could be related to O–O bonds (which typically have distance 2.6–2.7 Å) or even Ca-O (2.14 Å) may be a fit. Usually, Si-O and P-O distances are shorter (1.6–1.7 Å).

P13 contains SiO_2, $CaCO_3$, K_2SO_4, KCl, $Ca_5(PO_4)_3OH$ and γ-$Ca_3(PO_4)_2$. The lack of $K_2Ca(CO_3)_2$ and the higher amount of SiO_2 are consistent with its position in the K-MA class, where alkalis tend to associate with silicate and phosphate structures rather than carbonate phases.

P7 contains SiO_2 as the major phase, while K_2SO_4, KCl and $CaCO_3$ are also present. A weak set of reflections may correspond to $KAlSi_2O_6$, although this cannot be confirmed and is therefore considered tentative (marked "?" in Table 9). No phosphate phases are detected (possibly, they are present on a trace level). This phase composition reflects the SiO_2-rich character of the sample.

XRD pattern of sample P9 shows a distinct amorphous halo near 22°, indicating an amorphous SiO_2 matrix. Using Braggs' formula, this gives dominant distances ~4.04 Å. Elemental analysis shows that main component of ash is silica oxide. This dominate distance, most probably, is related to Si-Si bonds (~3.2 Å) in an oxygen-bridged tetrahedra Si-O-Si. However, observed longer distance indicates distorted structure (caused by the presence of large atoms, like K and Ca). The crystalline fraction consists of K_2SO_4, KCl and $(K,Na)_3Na(SO_4)_2$. No Ca-containing crystalline phases are present, consistent with the low CaO content.

TABLE 9. PHASE COMPOSITION OF BIOMASS ASH SAMPLES DETERMINED BY XRD

	Sample	**P12**	**P2**	**P4**	**P16**	**P8**	**P11**	**P15**	**P13**	**P7**	**P9**
	Class	**C**	**C-MA**	**CK**	**CK**	**CK**	**K**	**K**	**K-MA**	**S**	**S-MA**
COD number		Phase composition, wt.%									
9015390	$CaCO_3$ Calcite	72.7	65.8	13.1	22.2	44.4	5.6	–	16.5	6.4	–
9005017	SiO_2 Quartz (hexagonal)	5.1	11.8	–	–	1.7	–	–	28.7	70.3	–
9007569	K_2SO_4 Arcanite	8.6	9.3	24.8	37.9	14.2	14.7	–	18.6	15.4	28.3
1011242	$Ca_5(PO_4)_3(OH)$ Hydroxylapatite	13.6	13.1	16.0	5.9	39.7	28.8	–	19.9	–	–
9008300	$K_2Ca(CO_3)_2$ Fairchildite	–	–	46.0	33.9	–	22.5	–	–	–	–
1000050	KCl sylvite	–	–	–	–	–	1.0	–	6.3	7.9	26.7
IMA2001-070*	γ-$Ca_3(PO_4)_2$ Tuite	–	–	–	–	–	27.9	–	10.0	–	–
Pre-IMA-1813	$(K,Na)_3Na(SO_4)_2$ aphthitalite	–	–	–	–	–	–	–	–	–	45.0
Pre-IMA-1791	$KAlSi_2O_6$ leucite	–	–	–	–	–	–	–	–	?	–
–	Amorphous	–	–	–	–	–	+	+	–	–	+

* – International Mineralogical Association

4. CONCLUSION

The applied experimental approach, combined with the development of empirical models for dependent variables characterizing biomass combustion, demonstrates a transparent and comprehensible data analysis. The developed methodology can be applied in similar studies.

According to ISO 17225-6:2021, most of the pellets included in the study comply with specific classes:

- Class A: fully compliant pellets are P1, P2, and P3, while P4 is partially compliant due to low BD.
- Class B: partial compliance is observed for several pellets: P5 and P15 comply except for BD, P9 and P16 comply except for DU and BD, and P18 complies except for DU.
- Class C: fully or partially compliant pellets are P8, P12, P13, and P17.
- Pellets P4, P6, P7, P11, and P14 cannot be reasonably assigned to any class, as they fail in more than two criteria.

Considering the Commission Regulation (EU) 2015/1189 requirements for boilers using solid biomass fuels (including LQB pellets), it is appropriate to compare the minimum threshold values of the dependent variables with the measured results. The analysis shows that only P2 fully complies with the regulatory requirements. Pellets P4, P5, P13, P16, P17, and P18 completely fail to meet the criteria, indicating a potential limitation of LQB pellets as fuel for direct use in the private sector (e.g., household boilers), particularly given that the recommended fuel is defined by the manufacturer. For boiler manufacturers to safely designate LQB pellets as recommended fuel, boilers should be equipped with modifications that reduce emissions (e.g., PM [43]) and improve efficiency.

Also, high ash content had significant effect on pellet classification, which indicates the inaccurate proportion of biomasses in the pellet. These problems require further research, however data of the combustion tests could be used for modelling of predicament models for combustion processes like CFD modelling [44] and kinetic-based modelling [45].

Ashes of S, C-MA and K-MA types mostly form minerals that are less reactive and have high melting temperatures, stable during weathering and less mobile in water [37]. Indeed, samples P7 and P9 consist mainly of quartz, what can enhance an abrasion-erosion of combustion system. From another hand – recovering of some nutrients (like potassium chlorides and sulphates) can be done easier, as soon as the rest of the ash matrix is not soluble in water.

Ashes of C-MA, C and CK sub-types consist of minerals commonly unstable during weathering and have moderately soluble in water. They could be highly reactive with low decomposition temperatures, as described in [37]. In fact, calcium carbonate starts to decompose at around 750 °C [46]. Its high content in P2, P12, P8 may affect enhanced leaching behaviour, low-temperature transformations deposits formation and slagging [37]. However, ashes are suitable for production of different construction materials (e.g., cement additives) or for soil amendment [37].

Finally, ashes of K-MA, K and CK sub-types consist of minerals that are commonly unstable during weathering, and they are highly soluble in water, with low decomposition and melting temperatures during biomass combustion. As mentioned [37], they are responsible for enhanced leaching behaviour, low-temperature transformations, emission of volatile and hazardous elements, corrosion, deposits formation. Indeed, ash sample P15 is fully amorphous and P11 has high content of amorphous phase. At the same time, highly soluble minerals can serve as fertilizers or could be used to recover some trace elements from these types of ashes (minerals).

ACKNOWLEDGEMENT

This research was funded by the Latvian Council of Science, project “Alternative biomass knowledge for transition towards energy independence and climate targets (bioenergy Observatory)”, project No. lzp-2022/1-041.

REFERENCES

[1] Sertolli A., Gabnai Z., Lengyel P., Bai A. Biomass Potential and Utilization in Worldwide Research Trends – A Bibliometric Analysis. *Sustainability* 2022:14(9):5515. https://doi.org/10.3390/su14095515

[2] Svedovs O., Vīgants E., Siktars H., Kirsanovs V., Blumberga D. A Bibliometric and Literature-Based Overview of Biomass Pre-treatment and Conversion Technologies Modelling with Aspen Software. *Environmental and Climate Technologies* 2025:29(1):880–898. https://doi.org/10.2478/rtuect-2025-0059

[3] Ilari A., Duca D., Boakye-Yiadom K. A., Gasperini T., Toscano G. Carbon Footprint and Feedstock Quality of a Real Biomass Power Plant Fed with Forestry and Agricultural Residues. *Resources* 2022:11(2):7. https://doi.org/10.3390/resources11020007

[4] Park S., Kim S. J., Oh K. C., Kim S. Y., Kim H. E., Kim D. Predictive modelling of lignocellulosic biomass fuel changes during torrefaction via mass reduction. *J. Energy Inst.* 2025:118:101910. https://doi.org/10.1016/j.joei.2024.101910

[5] Sobamowo G. M., Ojolo S. J. Techno-Economic Analysis of Biomass Energy Utilization through Gasification Technology for Sustainable Energy Production and Economic Development in Nigeria. *Journal of Energy* 2018(1):1–16. https://doi.org/10.1155/2018/4860252

[6] Zeng Y. *et al.* Plasma-catalytic biogas reforming for hydrogen production over K-promoted Ni/Al_2O_3 catalysts: Effect of K-loading. *J. Energy Inst.* 2022:104:12–21. https://doi.org/10.1016/j.joei.2022.06.008

[7] González-Arias J., Baena-Moreno F. M., Gonzalez-Castaño M., Arellano-García H., Lichtfouse E., Zhang Z. Unprofitability of small biogas plants without subsidies in the Brandenburg region. *Environ. Chem. Lett.* 2021:19(2):1823–1829. https://doi.org/10.1007/s10311-020-01175-7

[8] Svedovs O., Sturmane A., Feofilovs M., Kirsanovs V., Romagnoli F. Comparative cradle-to-grave life cycle assessment of wood and alternative biomass pellet feedstocks for decentralized heating using experimental data. *Biomass Bioenergy* 2026:208:108880. https://doi.org/10.1016/j.biombioe.2025.108880

[9] Yao W., Zhao Y., Chen R., Wang M., Song W., Yu D. Emissions of Toxic Substances from Biomass Burning: A Review of Methods and Technical Influencing Factors. *Processes* 2023:11(3):853. https://doi.org/10.3390/pr11030853

[10] Kar T., Keles S. Environmental impacts of biomass combustion for heating and electricity generation. *Journal of Engineering Research and Applied Science* 2016:5(2):458–465.

[11] Bianchini A., Donini F., Pellegrini M., Rossi J., Saccani C. Innovative technological solutions moving towards the realization of a stand-alone biomass boiler with near-zero particulate emissions. *Energy Procedia* 2017:120:713–720. https://doi.org/10.1016/j.egypro.2017.07.198

[12] Svedovs O., Dzikevics M., Kirsanovs V., Veidenbergs I. A New Approach to Water Treatment: Investigating the Performance of Compact Particulate Matter Collector for Use in Compact Flue Gas Condenser. *Environmental and Climate Technologies* 2023:27(1):212–219. https://doi.org/10.2478/rtuect-2023-0016

[13] Blumberga D., Priedniece V., Kalniņš E., Kirsanovs V., Veidenbergs I. Small scale pellet boiler gas treatment in fog unit. *Int. J. Energy Environ. Eng.* 2021:12(2):191–202. https://doi.org/10.1007/s40095-020-00357-x

[14] Mawusi S. *et al.* A laboratory assessment of how biomass pellets could reduce indoor air pollution, mitigate climate change and benefit health compared to other solid fuels used in Ghana. *Energy Sustain. Dev.* 2023:72:127–138. https://doi.org/10.1016/j.esd.2022.12.011

[15] Shen G. *et al.* Reductions in Emissions of Carbonaceous Particulate Matter and Polycyclic Aromatic Hydrocarbons from Combustion of Biomass Pellets in Comparison with Raw Fuel Burning. *Environ. Sci. Technol.* 2012:46(11):6409–6416. https://doi.org/10.1021/es300369d

[16] Selivanovs J., Blumberga D., Ziemele J., Blumberga A., Barisa A. Research of Woody Biomass Drying Process in Pellet Production. *Environmental and Climate Technologies* 2012:10(1):46–50. https://doi.org/10.2478/v10145-012-0017-7

[17] Sommersacher P., Brunner T., Obernberger I. Fuel Indexes: A Novel Method for the Evaluation of Relevant Combustion Properties of New Biomass Fuels. *Energy Fuels* 2012:26(1):380–390. https://doi.org/10.1021/ef201282y

[18] Rocha S., Candia O., Valdebenito F., Flavio Espinoza-Monje J., Azócar L. Biomass quality index: Searching for suitable biomass as an energy source in Chile. *Fuel* 2020:264:116820. https://doi.org/10.1016/j.fuel.2019.116820

[19] Vasileiadou A., Zoras S., Iordanidis A. Fuel Quality Index and Fuel Quality Label: Two versatile tools for the objective evaluation of biomass/wastes with application in sustainable energy practices. *Environ. Technol. Innov.* 2021:23:101739. https://doi.org/10.1016/j.eti.2021.101739

[20] Nik Norizam N. N. A. *et al.* An improved index to predict the slagging propensity of woody biomass on high-temperature regions in utility boilers. *J. Energy Inst.* 2023:109:101272. https://doi.org/10.1016/j.joei.2023.101272

[21] Tian J. *et al.* A Biomass Combustion Chamber: Design, Evaluation, and a Case Study of Wheat Straw Combustion Emission Tests. *Aerosol Air Qual. Res.* 2015:15(5):2104–2114. https://doi.org/10.4209/aaqr.2015.03.0167

[22] Narnaware S., Pareek D. Performance Analysis of an Inverted Downdraft Biomass Gasifier Cookstove and its Impact on Rural Kitchen. *RERIC International Energy Journal* 2015:15(3):123–133.

[23] Anca-Couce A., Sommersacher P., Shiehnejadhesar A., Mehrabian R., Hochenauer C., Scharler R. CO/CO_2 ratio in biomass char oxidation. *Energy Procedia* 2017:120:238–245. https://doi.org/10.1016/j.egypro.2017.07.170
[24] Osei I., Kemausuor F., Commeh M. K., Akowuah J. O., Owusu-Takyi L. Design, Fabrication and Evaluation of Non-Continuous Inverted Downdraft Gasifier Stove Utilizing Rice husk as feedstock. *Scientific African* 2020:8:e00414. https://doi.org/10.1016/j.sciaf.2020.e00414
[25] Abdul Halim N. D. *et al.* The long-term assessment of air quality on an island in Malaysia. *Heliyon* 2018:4(12):e01054. https://doi.org/10.1016/j.heliyon.2018.e01054
[26] Al-Dabbous A. N. Diagnostic Ratios and Directional Analysis of Air Pollutants for Source Identification: A Global Perspective with Insights from Kuwait. *Atmosphere* 2025:16(9):1101. https://doi.org/10.3390/atmos16091101
[27] Nirel R., Dayan U. On the Ratio of Sulfur Dioxide to Nitrogen Oxides as an Indicator of Air Pollution Sources. *J. Appl. Meteorol. Clim*. 2001:40(7):1209–1222. https://doi.org/10.1175/1520-0450(2001)040<1209:OTROSD>2.0.CO;2
[28] Solid biofuels – Fuel specifications and classes, Part 6: Graded non-woody pellets. ISO. [Online]. [Accessed: 28.01.2025]. Available: https://www.iso.org/standard/76093.html
[29] Stelte W., Holm J. K., Sanadi A. R., Barsberg S., Ahrenfeldt J., Henriksen U. B. Fuel pellets from biomass: The importance of the pelletizing pressure and its dependency on the processing conditions. *Fuel* 2011:90(11):3285–3290. https://doi.org/10.1016/j.fuel.2011.05.011
[30] Gillespie G. D., Everard C. D., Fagan C. C., McDonnell K. P. Prediction of quality parameters of biomass pellets from proximate and ultimate analysis. *Fuel* 2013:111:771–777. https://doi.org/10.1016/j.fuel.2013.05.002
[31] Mojica-Cabeza C. D., García-Sánchez C. E., Silva-Rodríguez R., García-Sánchez L. A review of the different boiler efficiency calculation and modeling methodologies. *Inf. Téc.* 2021:86(1). https://doi.org/10.23850/22565035.3697
[32] Standard LVS EN ISO 16967:2015: Solid biofuels - Determination of major elements - Al, Ca, Fe, Mg, P, K, Si, Na and Ti. International Standard 2015.
[33] Standard LVS EN ISO 16968:2015: Solid biofuels - Determination of minor elements.
[34] D'Antonio M., Pendino V., Sinha S., Ciccarelli F. D. Network of Cancer Genes (NCG 3.0): integration and analysis of genetic and network properties of cancer genes. *Nucleic Acids Res.* 2012:40(D1):D978–D983. https://doi.org/10.1093/nar/gkr952
[35] Crystallography Open Database. [Online]. [Accessed 28.01.2025]. Available: https://www.crystallography.net/cod/
[36] Doebelin N., Kleeberg R. Profe: a graphical user interface for the Rietveld refinement program BGMN. *J. Appl. Crystallogr.* 2015:48(5):1573–1580. https://doi.org/10.1107/S1600576715014685
[37] Vassilev S. V., Vassileva C. G., Song Y.-C., Li W.-Y., Feng J. Ash contents and ash-forming elements of biomass and their significance for solid biofuel combustion. *Fuel* 2017:208:377–409. https://doi.org/10.1016/j.fuel.2017.07.036
[38] Vassilev S. V., Vassileva C. G., Vassilev V. S. Advantages and disadvantages of composition and properties of biomass in comparison with coal: An overview. *Fuel* 2015:158:330–350. https://doi.org/10.1016/j.fuel.2015.05.050
[39] Vassilev S. V., Baxter D., Andersen L. K., Vassileva C. G., Morgan T. J. An overview of the organic and inorganic phase composition of biomass. *Fuel* 2012:94:1–33. https://doi.org/10.1016/j.fuel.2011.09.030
[40] Kardaś D., Wantuła M., Pieter S., Kazimierski P. Effect of Separating Air into Primary and Secondary in an Integrated Burner Housing on Biomass Combustion. *Energies* 2024:17(18):4648. https://doi.org/10.3390/en17184648
[41] Bragg W. H., Bragg W. L. The reflection of X-rays by crystals. *Proc. R. Soc. Lond. Ser. Contain. Pap. Math. Phys. Character* 1913:88(605):428–438. https://doi.org/10.1098/rspa.1913.0040
[42] Fallah Z., Christie J. K. Molecular Dynamics Simulations of Binary Phosphate Glass Using the ReaxFF Potential. *J. Phys. Chem. B* 2024:128(46):11460–11467. https://doi.org/10.1021/acs.jpcb.4c04925
[43] Svedovs O., Dzikevics M., Kirsanovs V., Veidenbergs I. Development of New Compact Water Treatment System for Flue-Gas Condenser for Households. *Environ. Clim. Technol.* 2021:25(1):563–573. https://doi.org/10.2478/rtuect-2021-0041
[44] Zhang Z., He F., Zhang Y., Li X., Gao Z. Simulation of combustion process of a single biomass pellet based on heterogeneous-dimension discretization. *J. Energy Inst.* 2019:92(3):630–639. https://doi.org/10.1016/j.joei.2018.03.009
[45] Cao Y., Bai Y., Du J. H_2-rich gas production from co-gasification of biomass/plastics blends: A modeling approach. *J. Energy Inst.* 2024:112:101454. https://doi.org/10.1016/j.joei.2023.101454
[46] Karunadasa K. S. P., Manoratne C. H., Pitawala H. M. T. G. A., Rajapakse R. M. G. Thermal decomposition of calcium carbonate (calcite polymorph) as examined by in-situ high-temperature X-ray powder diffraction. *J. Phys. Chem. Solids* 2019:134:21–28. https://doi.org/10.1016/j.jpcs.2019.05.023